

# The Infrared Spectrum and Thermal Analysis of Zinc Hydroxide Nitrate

WALTER STÄHLIN AND HANS R. OSWALD

*Anorganisch-chemisches Institut der Universität Zürich,  
Rämistrasse 76, 8001 Zürich, Switzerland*

Received September 8, 1970

The infrared spectrum of zinc hydroxide nitrate,  $Zn_5(OH)_8(NO_3)_2 \cdot 2H_2O$ , is measured between 4000 and 20  $cm^{-1}$ . The data obtained by ir spectroscopy are compared with the results of the crystal structure determination. The thermal properties are established and the X-ray powder diagram of the dehydration product  $Zn_5(OH)_8(NO_3)_2$  is indexed with a monoclinic unit cell of the following dimensions:  $a = 17.92(1) \text{ \AA}$ ,  $b = 6.283(3) \text{ \AA}$ ,  $c = 5.391(2) \text{ \AA}$ , and  $\beta = 91.14(5)^\circ$ .

## Introduction

Feitknecht (1) described the synthesis of zinc hydroxide nitrate as a microcrystalline powder. Recently Stählin and Oswald (2) published the crystal structure determination of zinc hydroxide nitrate. The present paper reports on the infrared spectroscopical and thermal properties of



## The Infrared Spectrum of Zinc Hydroxide Nitrate

The spectra of zinc hydroxide nitrate and its partially (80%) deuterated analog were measured. The absorption bands are given in Table I.

The bands in the region of 3640 to 3310  $cm^{-1}$  are due to the OH stretching modes ( $\bar{\nu}OH$ ) of the hydroxide ions and the water molecules. The band shift of  $\bar{\nu}_H/\bar{\nu}_D = 1.36$  upon deuteration confirms this assumption. Nakamoto et al. (3) and other authors have found a relationship between the wavenumber of the absorption  $\bar{\nu}OH$  and the length of the hydrogen bond. Table II gives a comparison between the O-O distances as computed in the crystal structure analysis (2) and the values determined by infrared spectroscopy based on the paper of Nakamoto et al. (3). The agreement is quite satisfactory if one considers a probable error in bond-length determination of 2%.

The band at 1641  $cm^{-1}$  arises from the  $H_2O$  bending mode ( $\delta H_2O$ ). This assignment is supported by the shift  $\bar{\nu}_H/\bar{\nu}_D = 1.35$  which is found upon deuteration. The absorption occurs at slightly higher wavenumbers than in liquid water; this effect may

TABLE I

INFRARED SPECTRA OF  $Zn_5(OH)_8(NO_3)_2 \cdot 2H_2O$  AND  $Zn_5(OD)_8(NO_3)_2 \cdot 2D_2O$

$\bar{\nu}_H^b$ ( $cm^{-1}$ )		$\bar{\nu}_D^c$ ( $cm^{-1}$ )		$\bar{\nu}_H/\bar{\nu}_D$
3639	vw <sup>e</sup>	2684	w, sh	1.36
3580	w	2639	w, sh	1.36
3545	sho	2613	w, sh	1.36
3486	vs, b	2570	vs, b	1.35
3313	b, sho	2453	m, b	1.35
1641	s	1216 <sup>e</sup>	sho	1.35
1385	vs, b	1385	vs, b	
1055	w, sh	1055	w, sh	
817	w	817	w	
1017	w, b	738	w, b	1.38
893	m	679	m	1.32
841	w	609	vw, sho	1.38
764		552	vw, sho	1.36
644		489	vw, sho	1.32
523	w, b	522.5	w	
471.5	w, b	471.5	sho	
435	w, b	433	w, sho	
388.5	w, sho	388.5	w, sho	
326	w	323	w	
270	b, sho	266	w	

<sup>a</sup> This band is partially obscured by the absorption near 1385  $cm^{-1}$ .

<sup>b</sup>  $\bar{\nu}_H$  wavenumber for the absorption band of  $Zn_5(OH)_8(NO_3)_2 \cdot 2H_2O$ .

<sup>c</sup>  $\bar{\nu}_D$  same as above for  $Zn_5(OD)_8(NO_3)_2 \cdot 2D_2O$ .

<sup>e</sup> vw = very weak, w = weak, m = medium, s = strong, vs = very strong, sh = sharp, b = broad, sho = shoulder.

TABLE II  
HYDROGEN BOND LENGTHS IN  $Zn_5(OH)_8(NO_3)_2 \cdot 2H_2O$

Wavenumber (cm <sup>-1</sup> )	O-O distance (Å) ir	O-O distance (Å) crystal structure
3639	3.17	3.17
3580	3.03	3.06
3545	2.95	2.89
3486	2.88	2.84
3312	2.76	{2.75} {2.76}

be due to hydrogen bonding (Hartert (4)). The bands at 1385, 1055, and 817 cm<sup>-1</sup> are not sensitive to deuteration. They are attributed to modes of the nitrate ion.

In Table III the wavenumbers for the absorptions of different nitrates are compared with the values found for  $Zn_5(OH)_8(NO_3)_2 \cdot 2H_2O$ .

As the crystal structure determination for  $Zn_5(OH)_8(NO_3)_2 \cdot 2H_2O$  shows no evidence for direct bonding of the nitrate group to any of the cations, the band assignment was performed assuming the point symmetry  $D_{3h}$ . Yet the weak occurrence of the absorption  $\nu_1$ , which is ir forbidden for  $D_{3h}$  symmetry, together with the fact, that the absorption band  $\nu_3$  is rather broad, indicate that the symmetry is slightly lowered. But the deviation remains so little that the N-O distances, as determined in the crystal structure analysis, do not differ significantly one from the other and the absorption band at 1385 cm<sup>-1</sup>, which is due to the doubly degenerated mode  $\nu_3$ , does not split. A number of bands occurring between 1050 and 640 cm<sup>-1</sup> are shifted upon deuteration by a factor of 1.32 to 1.38. These bands may be due to OH bending modes  $\delta$  of MeOH, (Me stands for a metal ion).

Hartert and Glemser (7) have found that these modes occur at higher wavenumbers if the hydrogen

<sup>1</sup> Me stands for a metal ion.

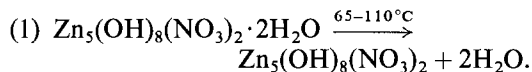
TABLE III  
MODES OF THE NITRATE ION

Compound	$\nu_1$	$\nu_2$	$\nu_3$	$\nu_4$	Ref.
NO <sub>3</sub> theoretical	1050	831	1390	720	(5)
KNO <sub>3</sub>	1052	826	1383	715	(6)
NaNO <sub>3</sub>		837	1381	725	(6)
$Zn_5(OH)_8(NO_3)_2 \cdot 2H_2O$	1055	817	1385	Not obsd	

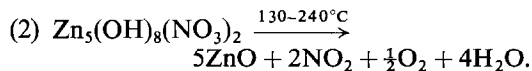
bond is stronger or if the Me-O distance is shorter. These authors calculate the apparent radius of the OH ion as a function of the  $\nu_{OH}$  and  $\delta_{MeOH}$  wavenumbers. Yet similar calculations for  $Zn_5(OH)_8(NO_3)_2 \cdot 2H_2O$  did not yield a convincing correlation with the values derived from the crystal structure. The model proposed by Hartert and Glemser (7) may be too simple for compounds containing different ligands and coordinations of the cations. The bands occurring below 530 cm<sup>-1</sup> are insensitive to deuteration, they are probably due to MeO stretching modes. The final assignment of the  $\delta_{MeOH}$  and  $\nu_{MeO}$  modes will be the subject of further investigations.

### Thermal Properties of Zinc Hydroxide Nitrate

Zinc hydroxide nitrate decomposes in two steps (Fig. 1):



Weight loss: theoretical, 5.78%; found, 5.3%.



Weight loss: theoretical, 28.91%; found, 28.5%.

The X-ray powder diffraction photographs show no detectable variation in the unit cell dimensions of zinc hydroxide nitrate between room temperature and 65°C. At a temperature of 110°C the powder diffraction diagram consists of the lines of  $Zn_5(OH)_8(NO_3)_2$ . The fully indexed powder diagram together with the unit cell dimensions are given in Table IV. At temperatures above 125°C, the first weak diffraction lines of zinc oxide can be detected together with some reflections of a further, not

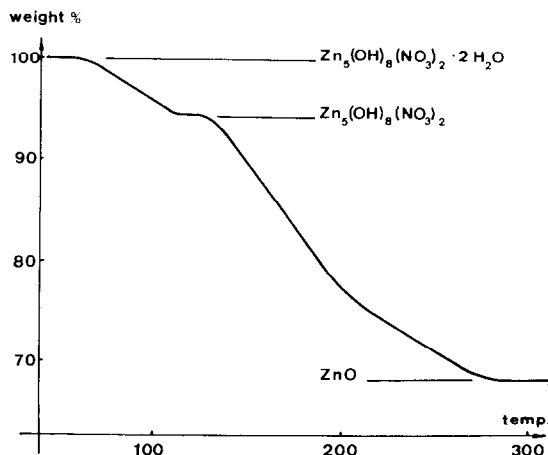


FIG. 1. Thermogravimetric curve for  $Zn_5(OH)_8(NO_3)_2 \cdot 2H_2O$ .

TABLE IV  
 X-RAY POWDER DIFFRACTION DATA OF  $Zn_5(OH)_8(NO_3)_2$ 

$I/I_0$	$d_{meas}$	$hkl$	$d_{calcd}$	$I/I_0$	$d_{meas}$	$hkl$	$d_{calcd}$
100	8.98	2 0 0	8.96				
27	5.93	1 1 0	5.93	4	2.330	{ 7 0 $\bar{1}$	2.331
15	5.17 b <sup>a</sup>	{ 1 0 $\bar{1}$	{ 5.19	17	2.309	{ 4 0 $\bar{2}$	2.330
		{ 1 0 1	{ 5.13	4	2.290	4 2 1	2.311
17	4.47	4 0 0	4.48	12	2.173	4 0 2	2.289
29	4.33	3 1 0	4.33	12	2.163	5 2 $\bar{1}$	2.174
43	4.10	0 1 1	4.09	3	2.080	6 2 0	2.165
9	4.04	3 0 $\bar{1}$	4.04	8	2.056	1 3 0	2.080
18	3.986 b	{ 1 1 $\bar{1}$	{ 4.002	12	2.029	5 1 $\bar{2}$	2.055
		{ 1 1 1	{ 3.976	10	1.998	1 2 2	2.029
10	3.762	2 1 $\bar{1}$	3.743	4	1.975	6 2 1	1.999
16	3.708	2 1 1	3.700	4	1.975	3 3 0	1.976
16	3.142	0 2 0	3.142	5	1.953	{ 0 3 1	{ 1.953
28	3.116	5 1 0	3.113	4	1.945	{ 8 1 1	{ 1.952
16	3.043	4 1 $\bar{1}$	3.044	2	1.910	3 2 $\bar{2}$	1.944
26	3.013	5 0 $\bar{1}$	3.012	2	1.910	2 3 $\bar{1}$	1.910
19	2.964 b	{ 2 2 0	{ 2.965	1	1.903	2 3 1	1.905
		{ 5 0 1	{ 2.957	15	1.872	{ 4 2 $\bar{2}$	{ 1.872
29	2.714	0 2 1	2.714	9	1.859	{ 7 2 $\bar{1}$	{ 1.872
68	2.688	1 2 $\bar{1}$	2.688	10	1.809	3 3 $\bar{1}$	1.860
11	2.607	2 2 $\bar{1}$	2.605	10	1.809	5 3 0	1.808
16	2.592	2 2 1	2.590	18	1.792	{ 10.00	{ 1.792
10	2.571	{ 4 2 0	{ 2.572	19	1.570	{ 1 0 $\bar{3}$	{ 1.791
		{ 2 0 2	{ 2.567	45	1.561	0 4 0	1.571
52	2.478	0 1 2	2.477	10	1.546	0 2 3	1.560
13	2.430	6 1 $\bar{1}$	2.430	15	1.393	2 4 0	1.547
13	2.401	2 1 $\bar{2}$	3.399	21	1.358	6 2 $\bar{3}$	1.392
10	2.371	7 1 0	2.371	12	1.343	1 3 $\bar{3}$	1.361
						1 0 $\bar{4}$	1.346

<sup>a</sup> b = broad. Only stronger reflections are tabulated below 1.79 Å.

Note: Unit cell dimensions:  $a = 17.92(1)$  Å,  $b = 6.283(3)$  Å,  $c = 5.391(2)$  Å, and  $\beta = 91.14(5)^\circ$ .  
 $V = 607.1(4)$  Å<sup>3</sup>; temperature,  $113 \pm 2^\circ\text{C}$ . (Values in parentheses are standard deviations.)

identified substance. If the temperature rises above  $150^\circ\text{C}$  the powder diagram consists of the broadened lines of zinc oxide only. As the temperature is elevated, the lines get gradually sharper due to recrystallization of zinc oxide. The discrepancy between the results of the thermal analysis and the high-temperature powder diffraction investigation in respect to the temperature at which the decomposition of zinc hydroxide nitrate to zinc oxide is completed,  $240$  and  $150^\circ\text{C}$ , respectively, can be explained as follows: The decomposition products  $\text{O}_2$ ,  $\text{NO}_2$ , and  $\text{H}_2\text{O}$  are adsorbed on the microcrystalline zinc oxide powder and are slowly released as the temperature rises and the zinc oxide recrystallizes; therefore, the weight loss is completed only at a temperature as high as  $240^\circ\text{C}$ .

The unit cell dimensions of the dehydration product mentioned in Table IV show a definite relation-

ship to the ones of  $Zn_5(OH)_8(NO_3)_2 \cdot 2\text{H}_2\text{O}$ , which are  $a = 19.480(5)$  Å,  $b = 6.238(1)$  Å,  $c = 5.517(1)$  Å, and  $\beta = 93.28(2)^\circ$ . The dimensions within the plane ( $b$ ,  $c$ ) are only slightly altered, therefore, the structure seems to collapse mainly along the direction normal to ( $b$ ,  $c$ ) during the loss of water molecules.

### Experimental

Single crystals of  $Zn_5(OH)_8(NO_3)_2 \cdot 2\text{H}_2\text{O}$  can be grown by precipitation from homogeneous solution of zinc nitrate ( $2 M$  in water) with urea ( $2\text{--}3 M$ ) at  $63^\circ\text{C}$ . The solution is stirred slowly and a stream of nitrogen is bubbled through it to remove the carbon dioxide produced in the decomposition of urea. The yield is very low ( $5\%$ ) because the reaction has to be interrupted after 24 hr to prevent the deposition of microcrystalline products. The crystals are

rhomb-shaped and of the following average dimensions:  $0.2 \times 0.2 \times 0.03$  mm.

Infrared spectra were measured with a Beckman IR-12 spectrometer in the region of 4000 to  $400\text{ cm}^{-1}$  in KBr and in the region from 1500 to  $200\text{ cm}^{-1}$  in CsI pellets.

The thermal analysis was accomplished with a Mettler Thermoanalyzer (Mettler, Switzerland). Samples of 4 to 10 mg were heated in a platinum crucible in a stream of dry air of atmospheric pressure with a heating rate of  $1^\circ\text{C}/\text{min}$ . The products were identified by X-ray powder diffraction.

X-ray powder diagrams were taken on a focusing camera of the Guinier de Wolff type (Nonius, Delft) with  $\text{Cu } K_\alpha$  or  $\text{Fe } K_\alpha$  radiation. High purity potassium chloride was used as an internal standard for the determination of accurate lattice spacings. The unit cell dimensions were refined by least-squares calculations.

High-temperature X-ray powder photographs were obtained with a Guinier-Lenne camera (Nonius, Delft) with  $\text{Cu } K_\alpha$  radiation. The sample was heated in air with a heating rate of  $0.5^\circ\text{C}/\text{min}$ .

Single crystal X-ray photographs were taken on a Weissenberg goniometer (Nonius, Delft) with  $\text{Cu } K_\alpha$  radiation (Ni filter) and a Buerger precession

camera (Supper, USA) with  $\text{Mo } K_\alpha$  radiation (Zr filter).

X-ray diffraction intensities were recorded photographically and measured with a double-beam microdensitometer (Joyce-Loebl mark III CS).

### Acknowledgment

This research has been supported by the Schweizerischer Nationalfonds zur Förderung der wissenschaftlichen Forschung, project number 2.131.69.

### References

1. W. FEITKNECHT, *Helv. Chim. Acta* **16**, 427 (1933).
2. W. STÄHLIN AND H. R. OSWALD, *Acta Crystallogr., Sect. B.* **26**, 860 (1970).
3. K. NAKAMOTO, M. MARGOSHES, AND R. E. RUNDLE, *J. Amer. Chem. Soc.* **77**, 6480 (1955).
4. E. HARTERT, *Naturwissenschaften* **43**, 275 (1956).
5. G. HERZBERG, "Infrared and Raman Spectra of Polyatomic Molecules," Van Nostrand, Princeton, N.J., 1945.
6. K. BUIJS AND C. J. H. SCHUTKE, *Spectrochim. Acta* **18**, 307 (1962).
7. E. HARTERT AND O. GLEMSER, *Z. Elektrochem.* **60**, 746 (1956).